HHS Public Access

Author manuscript

Osteoarthritis Cartilage. Author manuscript; available in PMC 2020 November 01.

Published in final edited form as:

Osteoarthritis Cartilage. 2019 November ; 27(11): 1669–1679. doi:10.1016/j.joca.2019.07.012.

THE NOCICEPTIVE INNERVATION OF THE NORMAL AND OSTEOARTHRITIC MOUSE KNEE

Alia M. Obeidat, MS[1], **Rachel E. Miller, PhD**[1], **Richard J. Miller, PhD**[2], **Anne-Marie Malfait, MD, PhD**[1]

[1]Department of Internal Medicine, Division of Rheumatology, Rush University Medical Center, Chicago IL

[2]Department of Pharmacology, Northwestern University, Chicago IL

Abstract

Objectives—To document the nociceptive innervation of the normal and osteoarthritic murine knee.

Methods—Knees were collected from naïve male C57BL/6 $Na_V1.8$-tdTomato reporter mice aged 10, 26, and 52 weeks (n=5/group). Destabilization of the medial meniscus (DMM) or sham surgeries (n=5/group) were performed in the right knee of 10-week old male $Na_V1.8$-tdTomato mice, and knees were harvested 16 weeks later. Twenty 20-μm frozen sections from a 400-μm mid-joint region were collected for confocal microscopy. Integrated density of the tdTomato signal was calculated using Image J by two independent observers blinded to the groups. Consecutive sections were stained with hematoxylin & eosin. C57BL/6-Pirt-GCaMP3 mice (n=5/group) and protein gene product 9.5 (PGP9.5) immunostaining of C57BL/6 wild type (WT) mice (n=5/group) were used to confirm innervation patterns.

Results—In naive 10-week old mice, nociceptive innervation was most dense in bone marrow cavities, lateral synovium and at the insertions of the cruciate ligaments. By age 26 weeks, unoperated knees showed a marked decline in nociceptors in the lateral synovium and cruciate ligament insertions. No further decline was observed by age 1 year. Sixteen weeks after DMM, the medial compartment of OA knees exhibited striking changes in $Na_V1.8$+ innervation, including increased innervation of the medial synovium and meniscus, and nociceptors in subchondral bone channels. All results were confirmed through quantification, also in Pirt-GCaMP3 and PGP9.5-immunostained WT mice.

Corresponding author: Rush University Medical Center, 1611 W Harrison Street, suite 510, 60612 Chicago IL, anne-marie_malfait@rush.edu, Tel: 1-312 563 2925, Fax: 1-312-563-2267.

Author contributions:

Alia Obeidat: Acquisition, analysis and interpretation of data. Drafting of the manuscript.

Rachel Miller: Analysis and interpretation of data. Drafting of the manuscript.

Richard Miller: Analysis and interpretation of data. Drafting of the manuscript.

Anne Marie Malfait: Analysis and interpretation of data. Drafting of the manuscript.

All authors approved the final version of the manuscript.

Conflicts: A.M. Malfait serves as an Associate Editor for Osteoarthritis and Cartilage.

Conclusions—Nociceptive innervation of the mouse knee markedly declines by age 26 weeks, before onset of spontaneous OA. Late-stage surgically induced OA is associated with striking plasticity of joint afferents in the medial compartment of the knee.

Keywords

Knee joint; $Na_V1.8$; nociceptors; osteoarthritis; mouse; innervation

Osteoarthritis (OA) is the most common form of arthritis in the knee, affecting millions of people worldwide (1). It is the most frequent cause of joint pain, and pain is one of the most significant clinical problems in OA. Mechanisms of OA pain remain poorly understood, but there is compelling clinical evidence to suggest that ongoing peripheral input from the affected joint drives OA pain (2).

It is not known which structures in an osteoarthritic joint give rise to pain. OA was long considered a disease of degenerating cartilage, and cartilage is aneural (3). In recent years, concepts of OA pathogenesis have evolved to suggest that OA represents the failure of the joint as an organ. Pathological changes in individual joint tissues, including cartilage, subchondral bone, synovium, meniscus – and, crucially, the crosstalk between them - contribute to disease progression and pain (4, 5). Within this “organ failure” concept, involvement of the intra-articular sensory innervation remains a largely unanswered question. Importantly, we do not know whether knee innervation associated with OA pain is different from the normal knee. Therapeutic advances for OA pain must clearly be targeted to the pathological situation.

In order to enhance our understanding of the role of sensory innervation in OA joint pain, we need to elucidate the anatomical distribution of sensory neurons inside the joint. Currently, detailed information on intra-articular sensory innervation is lacking, and this is true for normal, healthy joints as well as joints affected by OA (reviewed in 6). Light and electron microscopy studies have shown that many joint tissues are richly innervated by sensory (80% nociceptors) and sympathetic nerves, including the capsule, ligaments, menisci, periosteum and subchondral bone (3, 7–11). However, precise information on the anatomical distribution of free nerve endings in the knee, and how this is affected by OA joint remodeling is lacking.

Hence, we aimed to document the nociceptive innervation of the mouse knee using $Na_V1.8$-tdTomato reporter mice (12), which express a bright red fluorescent tdTomato reporter in all neurons that express the voltage-gated sodium channel, $Na_V1.8$. This neuronal subset comprises approximately 75% of dorsal root ganglion (DRG) sensory neurons, including >90% of C-nociceptors, as well as a small fraction of Aδ-nociceptors and Aβ afferents (13). C-fibers can be subdivided in two distinct subsets, which innervate distinct peripheral tissues, and subserve different functional modalities: peptidergic C-fibers, which secrete neuropeptides, including calcitonin-gene related peptide (CGRP) and substance P, and non-peptidergic C-fibers, which do not secrete these neuropeptides and are characterized though binding of IB4 (14). Shields *et al.* characterized the $Na_V1.8$-Cre-positive neuronal population extensively and found that CGRP-positive neurons make up more than 50% of $Na_V1.8$-Cre-positive neurons, while approximately half of the $Na_V1.8$-Cre-positive neurons

bind IB4 (13). Therefore, in order to study the nociceptive innervation of the mouse knee, we focused on the $Na_V1.8+$ population. Using a molecular genetic strategy of crossing $Na_V1.8$-Cre mice (15) with Ai9 (td-Tomato) mice (16) resulted in $Na_V1.8$-Cre;Ai9 mice ("$Na_V1.8$-tdTomato reporter mice"), in which $Na_V1.8$-positive DRG neurons are labeled red with td-Tomato reporter protein following Cre-dependent recombination. These mice enable us to visualize $Na_V1.8$-positive neuronal cell bodies and their afferents as we have previously validated in the DRG, the dorsal horn and the skin of these mice (17).

We used these $Na_V1.8$-tdTomato reporter mice to describe the intra-articular nociceptive innervation of the ageing mouse knee. Furthermore, we explored if changes occur in a model of OA, induced by destabilization of the medial meniscus (DMM) in order to provide an anatomical context for our understanding of OA-related pain.

MATERIALS AND METHODS

Animals

We used a total of n= 66 male mice. All animal procedures were approved by the Institutional Animal Care and Use Committee at Rush University Medical Center. Animals were housed with food and water *ad libitum* and kept on 12-hour light cycles. $Na_V1.8$-tdTomato C57BL/6 reporter mice were a gift from Dr. John Wood, University College London, London, UK (13, 15). Pirt-GCaMP3 mice on a C57BL/6 background were provided by Dr. Xinzhong Dong, Johns Hopkins University School of Medicine, Baltimore, USA (18). Pirt-GCaMP3 mice express the fluorescent calcium indicator, GCaMP3, in ~90% of all sensory DRG neurons, and not in other peripheral or central tissues, through the Pirt promoter (18–20). Wild type (WT) C57BL/6 mice were inbred at Rush.

Destabilization of the medial meniscus (DMM)

Mice were randomized by litter to DMM or sham surgery. DMM or sham surgery was performed in the right knee of 10-week-old male mice, as described (21, 22). For details, see Suppl. Methods.

Mechanical allodynia

Mechanical allodynia in the ipsilateral hind paw was tested by a blinded observer who evaluated sensitivity to von Frey monofilaments, using the up-down staircase method of Dixon (23, 24), as described (22). Details are in Suppl. Methods.

DRG Histology

L4 lumbar DRG was harvested from a 10-week old mouse. Twelve-μm thick cryosections were cut throughout the DRG, and imaged using a laser-scanning confocal microscope (Olympus IX70).

Knee Histology

Mice were anesthetized by ketamine and xylazine and perfused transcardially with phosphate buffered saline (PBS) followed by 4% paraformaldehyde in PBS (25). For studies in naïve $Na_V1.8$-tdTomato mice, right knees were collected at age 10 weeks (n=6), 26 weeks

(n=5), and 1 year (n=5). For experimental OA studies, knees were collected 16 weeks after sham (n=5) or DMM (n=5) surgery. For Pirt-GCaMP3 mice, we collected right knees at 10 weeks (n=5), 26 weeks (n=5) and 1 year (n=3), as well as 16 weeks after DMM (n=5). WT knees (used for PGP9.5 immunohistochemistry) were collected 10 weeks (n=5), 26 weeks (n=5) and 16 weeks after DMM (n=5). A sample size of 5 for all groups was chosen based on previous data and assuming a power of 0.8 to differentiate OA joint damage at 16 weeks *post* DMM (mean±SD 13±5) from naïve (1.2±1.3) and sham (0±0) controls. Assuming an ANOVA method to compare 3 groups with a standard deviation of 5 for all groups, statistical significance level α=0.05, power =0.8 we calculated that we would need 4 mice per group using G*Power 3.1 for Mac. For sample preparation, see Suppl. Methods. Twenty-μm thick coronal sections were cut throughout the whole joint using the cryostat as follows (Supplemental Fig. 1): the first 400-μm thick area comprises the anterior covering of the knee joint and includes the patella and attached patellar tendon. The next fifty sections (1000-μm thick area) comprise the anterior region of the articular cavity (A in Supplemental Fig. 1 marks the end of that area) and defined as the area where at least one of the meniscal horns (medial, lateral or both) has a ligament attached to it. The mid-joint region comprises the next twenty sections from an approximately 400-μm thick region (area B in Supplemental Fig. 1). The start of the mid-joint region was defined as the area where the meniscal horn is devoid of any ligament attachments. We focused on sections from this region for all histological and histopathological analyses in this study, because this is the region where the majority of the cartilage damage develops in the DMM model (21). The final region is the posterior region of the articular cavity (C in Supplemental Fig. 1 marks the beginning of the posterior region). Sections from the mid-joint region were imaged using either a laser-scanning confocal microscope (Olympus IX70) or Nikon A1R Confocal Laser Microscope. Consecutive sections were stained with hematoxylin (1x-Sigma HHS160) and eosin (1%-Sigma E4382) (H&E), or toluidine blue (0.04% w/v), using standard methods. Images were then processed using Image J and Fluoview software (FV10-ASW 4.2 Viewer). Adjustments were made to brightness and contrast to reflect true colors (25). All images were treated exactly the same in terms of adjustments to brightness and contrast to minimize bias. In addition, one knee from a 10-week old naïve mouse and one knee from a mouse 16 weeks after DMM were imaged using a Nikon A1R Confocal Laser Microscope, which provides high-quality confocal images at ultrahigh-speed, enhancing sensitivity and minimizing autofluorescence.

In order to make sure that the tdTomato signal seen in $Na_V1.8$-tdTomato sections does not reflect autofluorescence, we imaged the right knees from three 10-week old male WT mice using the confocal microscope (Olympus IX70), using the same laser power as for the $Na_V1.8$-tdTomato mice. Images were processed with the same settings as their $Na_V1.8$ counterparts. Minimal signal was seen in these WT sections (Supplemental Fig. 2), indicating that tissue autofluorescence is not impacting interpretation of the $Na_V1.8$-tdTomato images.

Immunohistochemistry

Knees from WT mice (20-μm frozen sections) were stained for the pan-neuronal marker, protein gene product 9.5 (PGP9.5) (26–28). Detailed methods are described in Suppl.

Methods. In order to show the overlap between $Na_V1.8$ tdTomato and PGP9.5 signal, 20-μm frozen knee sections from 10-week old naive $Na_V1.8$ tdTomato mice (n=2) were immunostained for PGP9.5, using the same staining protocol as for WT sections.

Histopathology of the knee

H&E stained sections, consecutive to the ones used for confocal imaging, were evaluated for cartilage degeneration, based on modified Osteoarthritis Research Society International recommendations (29). For details, please see Suppl. Methods.

Quantification of the $Na_V1.8$-tdTomato signal

The $Na_V1.8$+ signal in the medial and lateral synovium and the cruciate ligaments was quantified by calculating the integrated densities of these areas using Image J. Within the mid-joint region, the section with maximal signal was chosen for each knee. Regions of interest (ROI) were outlined for each section and quantified in Image J (Suppl. Fig. 3). On the lateral side, a region including both the synovium and meniscus was outlined (Suppl. Fig. 3a). For the cruciates, a region containing both the anterior and posterior cruciate ligaments was outlined (Suppl. Fig. 3b). On the medial side, the junction of the inner and outer meniscus was delineated. The outer and inner regions have a different histological aspect and thus using the phase contrast images a line was drawn between these areas, and a standardized area on the outer side of this line was outlined for knees from all groups. The ROIs were saved and used to mark the same area on the corresponding $Na_V1.8$ images (Suppl. Fig. 3c). Finally, an area of the medial synovium adjacent to the capsule was outlined (Suppl. Fig. 3d).

Channels observed in the subchondral bone of the medial femoral condyles and tibial plateaux that contained $Na_V1.8$+ nerves were quantified as follows: two mid-joint sections (80 μm apart) per knee were used to count $Na_V1.8$+ channels; counts were averaged for each knee and compared with shams and age-matched naïve mice.

Quantification procedures were similar for sections from Pirt-GCaMP3 mice and PGP9.5 immunostained WT mice. All quantifications were independently calculated by 2 independent observers (AO and REM), blinded to the groups. The intraclass correlation (ICC) was > 0.91, indicating very good agreement between both assessors. Therefore, the average scores of AO and REM quantifications are presented.

Statistical Analysis

For each tissue and for each line of mice, the average scores of the two assessors were assessed for normality using the Kolmogorov-Smirnov normality test and data were log-transformed data if necessary (only the $Na_V1.8$-tdTomato ligament data were log transformed). One-way ANOVA was used to compare the scores for a particular tissue compartment for either $Na_V1.8$-tdTomato mice, Pirt-GCaMP3, or PGP9.5 immunostaining in WT mice. If the one-way ANOVA was significant ($p < 0.05$), Tukey post-hoc tests were performed. For $Na_V1.8$-tdTomato post-hoc tests, please see Suppl. Methods.

RESULTS

$Na_V1.8$ distribution in the knees of 10-week and 26-week old mice

First, we validated that the $Na_V1.8$ signal was present in the L4 DRG. One example of a confocal micrograph of an L4 DRG harvested from a $Na_V1.8$ tdTomato reporter mouse showed that $Na_V1.8$-positive cell bodies are all small-to-medium sized, consistent with nociceptors (Supplemental Fig. 4).

These mice were then used for analysis of knee innervation. Fig. 1a shows H&E staining of a coronal section through the mid-joint of a 10-week old healthy knee. Consecutive sections revealed areas of dense innervation by $Na_V1.8$+ nerves. These areas were, most notably, the lateral synovium (Fig. 1b,c), the connective tissue layer (the epiligament) surrounding the cruciate ligaments, and the insertion sites of the cruciate ligaments (Fig. 1d,e). Furthermore, bone marrow cavities were also densely innervated (Fig. 1b, c and detailed in Suppl. Fig. 5). Imaging with a Nikon A1R Confocal microscope showed the dense innervation in the lateral synovium at higher magnification (Fig. 2a,b). The synovium in the medial compartment (including superficial and deep layers of the synovium) (Fig. 1f,g) and the collagenous substance of the cruciate ligaments were less densely innervated (Fig. 1d,e). Articular cartilage, lateral and medial meniscus showed no fluorescent signal.

Fig. 3 shows a representative 26-week old mouse knee. At this age, knees showed no signs of OA (for n=5 mice, the cartilage degeneration score was 0.2±0.4 (mean±SD), concordant with previous findings (22)) (Fig. 3a). Analysis of the $Na_V1.8$+ signal revealed a sharp decline in the innervation of the lateral synovium (Fig. 3b,c), as well as in the epiligament and the insertions of the cruciate ligaments (Fig. 3d,e) compared to 10-week old knees.

We quantified the fluorescent signal of mid-knee coronal sections from 10-week old (n=6), 26-week old (n=5) and 1-year old (n=5) mice, and found remarkably reproducible patterns within the different age-groups, confirming a marked decline in innervation of the lateral synovium (Fig. 4a) and the cruciate ligaments (Fig. 4b), in 26-week old mice compared to 10-week old mice. No further decline was observed in the knees from 1-year old mice (Fig. 4a,b). The innervation in the medial synovium was low in all three age groups and there was no difference in the fluorescence levels among these groups (Fig. 4c). For all comparisons, the mean difference and 95% CI of the difference are reported in Supplemental Table 1.

Changes in $Na_V1.8$ distribution 16 weeks after DMM

We performed DMM (n=5) or sham (n=5) surgery in 10-week old male $Na_V1.8$-tdTomato reporter mice. First, we wanted to make sure that these $Na_V1.8$-tdTomato reporter mice behave similarly to WT mice after DMM, with respect to joint damage and presence of mechanical allodynia. Indeed, we confirmed that, by 16 weeks after DMM, these mice had OA joint damage (cartilage degeneration score after DMM=12.8 ± 1.9, compared to 0.4±0.49 after sham surgery, mean±SD, $p<0.0001$), comparable to WT mice (22). Fig. 5 shows a representative knee 16 weeks after DMM. H&E staining revealed marked OA-like changes in the medial compartment, including cartilage loss, subchondral bone sclerosis, and osteophyte formation (Fig. 5a). Associated with OA joint damage, these mice also showed mechanical allodynia levels similar to WT DMM mice (50% withdrawal thresholds

in the hind paw: 0.032 ± 0.008g (n=5) *vs.* naive base line: 0.565 ± 0.054g (n=6), mean±SD p<0.0001).

Sixteen weeks after DMM, we observed no changes in $Na_V1.8$+ signal in the lateral synovium (Fig. 5b,c) and the cruciate ligaments (Fig. 5d,e); quantification shown in (Supplemental Fig. 6 a,b). In contrast, we detected a clear $Na_V1.8$+ fluorescent signal in the deep layers of the synovium of the medial compartment, while no change was observed in the synovial lining layer (Fig. 5f,g, blue arrows; for higher magnification, see Fig. 6). Quantification of the medial synovium revealed increased innervation 16 weeks after DMM, compared to sham-operated mice or age-matched naïve controls (Fig. 6b). $Na_V1.8$+ fluorescence was also observed in the outer region of the medial meniscus, close to the junction of the outer and inner areas (Fig. 6a). Quantification of this signal showed increased innervation after DMM, compared to shams and naïve age-matched controls (Fig. 6c) (Suppl. Table 1). These changes were confirmed using a Nikon A1R confocal microscope, which clearly showed the nerves on the medial side (Fig. 6d,e), and the signal within the medial meniscus (Fig. 6d,f).

In addition to increased innervation of the medial synovium and meniscus, major changes occurred in the $Na_V1.8$+ innervation of the subchondral bone in the medial compartment. Most strikingly, we noted remodeling in the sclerotic subchondral bone, where $Na_V1.8$+ nociceptors were observed pointing toward calcified cartilage (Fig. 7a,b). Quantification of the number of $Na_V1.8$+ subchondral bone channels in tibial plateaux and femoral condyles from 26-week old naïve mice, and 16 weeks after sham or DMM surgery (Fig. 7c) revealed a marked increase in OA knees (Suppl. Table 1). The subchondral bone channels were also observed using the Nikon A1R confocal microscope (Fig. 7d,e). $Na_V1.8$ nociceptors were also present in osteophytes (Suppl. Fig. 7).

Validation of the findings in Pirt-GCaMP3 mice and by PGP9.5 staining in WT mice

Since the current study is the first attempt to use $Na_V1.8$-tdTomato reporter mice to study joint innervation, we sought to independently confirm innervation patterns using pan-sensory neuronal markers. We analyzed knees of Pirt-GCaMP3 mice, where all DRG neurons are labelled green, at ages 10 weeks (n=5), 26 weeks (n=5) and 1 year (n=3), as well as 16 weeks after DMM (n=5). Ten-week old Pirt-GCaMP3 knees showed a similar neuroanatomical distribution of nerves to 10-week old $Na_V1.8$-tdTomato mice (Supplemental Fig. 8a–c). In addition, at 26 weeks, a clear decline was observed in the GCaMP3 positive nerve fibers innervating the lateral synovium and cruciate ligaments insertions (Suppl. Fig. 8d–f). We also analyzed Pirt-GCaMP3 knees 16 weeks after DMM (n=5) and observed a similar pattern of innervation to $Na_V1.8$ tdTomato reporter mice: GCaMP3+ fibers in channels in the subchondral bone of the medial compartment (Suppl. Fig. 9a, magnified in b), increased innervation of the medial synovium (Suppl. Fig. 9a, magnified in c), and GCaMP3+ signal in the medial meniscus (Suppl. Fig. 9c). Quantification of the signals from Pirt-GCaMP3 mice is shown in Fig. 8a (Suppl. Table 1).

As a final test of the observations we have made, we analyzed PGP9.5 immunostaining in the knees of WT mice, 10-week old naïve mice (n=5), 26-week old naïve mice (n=5), and 16 weeks after DMM (n=5), again confirming the observations made in $Na_V1.8$-tdTomato mice

(Supplemental Fig. 10 and Fig. 11). Quantifications are shown in Fig. 8b (Suppl. Table 1). No primary antibody control images are shown in Suppl. Fig. 12.

Lastly, we immunostained knee sections from 2 naïve 10-week old $Na_V1.8$-tdTomato mice for PGP9.5, and showed that all $Na_V1.8$ fibers stained positively for this pan-neuronal marker, further strengthening the observations (Suppl. Fig. 13).

DISCUSSION

The availability of $Na_V1.8$-tdTomato fluorescent reporter mice provided us with an unprecedented opportunity to study the nociceptive innervation of the murine knee. The $Na_V1.8$ voltage-dependent sodium channel is uniquely expressed by 75% percent of DRG neurons, including the majority of nociceptors (13). One advantage of studying the mouse knee is that it is small enough to be sectioned intact, thereby giving an overview of the entire knee. In 10-week old mice, we found that $Na_V1.8$ neurons densely innervated bone marrow cavities, which confirms reports in the literature that bone marrow is densely innervated by both Aδ- and C-fiber sensory neurons (30). It receives the greatest total number of sensory and sympathetic neurons when compared to mineralized bone and periosteum (31, 32). Intra-articular innervation was most pronounced in the lateral synovium, the connective tissue layer surrounding the cruciate ligaments, and their insertion sites. $Na_V1.8$+ nociceptors were also visible at the margin of the outer edge of the lateral meniscus. The medial synovium and the collagenous substance of the cruciate ligaments were less densely innervated. Articular cartilage, medial meniscus and lateral meniscus did not show innervation. These findings in 10-week old mice confirm the anatomical literature on knee joint innervation, where it has been described that free nerve endings are found in all joint tissues, including the fibrous capsule, fat, menisci, and ligaments, but not in articular cartilage (3).

The most striking, and perhaps unexpected, finding was the sharp decline in $Na_V1.8$+ neurons in the knees of 26-week old mice. It is known that both morphology and function of the peripheral nervous system dramatically change with age. In several species, including humans and mice, analysis of peripheral nerves such as the peroneal, sural, and tibial nerves has revealed an age-dependent reduction in number and density of myelinated fibers, and a loss of unmyelinated fibers (33). Furthermore, it has been reported that nerve fiber loss in ageing mice involves unmyelinated fibers more markedly than myelinated fibers (34).

Information on the abundance of free nerve endings in peripheral tissues with age is limited. In human skin, an age-related linear reduction of the sensory innervation of the epidermis of the forearms and legs has been reported, commencing in adulthood (35). This is compatible with reports of decreased sensitivity to mechanical stimuli in the elderly (36). There is even less information on the abundance of free nerve endings in ageing joints. A study of human menisci demonstrated a decrease of about 70% of free nerve endings in menisci from people over 60 (37). Age-related changes in sensory innervation of the mouse knee have not yet been reported. One group investigated the numbers of DRG cell bodies retrogradely labeled with Fluorogold injected into the knee joint cavity, and found a loss of afferents from knee joints, mostly during the first third of the lifespan of the mouse (38, 39). Over the lifespan of

the mouse (2 years), DRG cell bodies innervating the knee declined about 57%, and this occurred in two phases: a rapid loss over the first 8 months of life and a slower rate over the remaining months (38).

These findings are in concordance with current observations demonstrating a marked decline in sensory innervation of the murine knee between the ages of 10 and 26 weeks. Remarkably, this loss of innervation occurs quite early on in the life of the mouse, with a steep decline by age 26 weeks, and no further decline by 1 year. In contrast, there was no change in $Na_V1.8$ signal in bone marrow cavities with age, confirming a recent report that analyzed CGRP-positive neurons in bone marrow cavities of ageing mouse femora (40). It is noteworthy that in the study by Salo *et al.* (39), as in the current study, decline of sensory innervation preceded onset of cartilage degeneration. Indeed, at 26 weeks, mice had no signs of OA, as reported before (41). The biological significance of this is not clear at this time, but it has been reported that crude de-afferentiation, for example through “DRG-ectomy” or killing nerves with an intra-articular neurotoxin, can either initiate or accelerate OA-like joint damage (39, 42). Therefore, it is possible that loss of sensory innervation renders the joint vulnerable to damage and may be a pathogenic factor in age-related OA. Future work will address this hypothesis.

It is interesting to discuss our findings in the context of a unique experiment by Dye *et al.*, who gallantly attempted to map the conscious neurosensory characteristics of the human knee by arthroscopic palpation of the knee of one of the authors, without intra-articular anesthesia (43). They reported moderate or severe pain upon palpation of the anterolateral synovium and anterior fat pad. The mid-region of the cruciate ligaments elicited only slight discomfort, but pain increased markedly at their femoral and tibial insertion points. Touching the capsular margins of the menisci elicited moderate pain, especially at the lateral meniscus, while the inner meniscal rims were not painful. Therefore, this anecdotal study on pain sensation in the human knee is concordant with our findings on nociceptors distribution in the healthy mouse knee.

Next, in order to analyze which structures in the osteoarthritic joint may contribute to pain, we studied changes in nociceptive innervation 16 weeks after DMM, at which time mice have severe OA and associated mechanical allodynia. We observed striking changes in sensory innervation after DMM, particularly in the medial compartment of the knee, where OA joint damage occurs. These changes included increased innervation in the medial synovium, and the appearance of nociceptors in channel-like structures present in the subchondral bone. Nociceptors were also observed within the medial meniscus, close to the junction of outer and inner regions, and in osteophytes.

The literature on structural changes in knee innervation in OA is scant, but compatible with the current murine findings. In human OA knees, vascular penetration and nerve growth have been described in osteophytes (44), in subchondral bone (45), and in the meniscus (46). In the human meniscus, CGRP+ nerves (*i.e.,* peptidergic C-fibers) have been described in the outer regions of the medial meniscus, in association with small arterioles (46). Furthermore, vascular channels that breach the tidemark between subchondral bone and articular cartilage may contain sympathetic and sensory nerves (44, 47). These channels

have also been described in animal models of OA, for example after rat meniscectomy, where it has been proposed they may represent a source of pain (48).

Reports on innervation of the synovium in OA joints are very limited and in contrast to our current findings. Two studies have examined murine knee innervation in the collagenase-induced model, and found either a transient (49) or permanent (50) decrease in sensory innervation in the synovium, particularly peptidergic fibers. In the rat monoiodoacetate (MIA) model, two studies examined the number of DRG neurons retrogradely labeled from the knee, and both found a significant reduction (51, 52), but it is not clear if this was part of OA pathology or a neurotoxic effect of MIA (53). In human OA knees, inflamed synovium exhibited a significant decrease of CGRP+ and TH+ nerve density close to the synovial lining layer, whereas deeper layers were less affected (26). In contrast, we report an increase of nociceptors in the deeper layers of the medial synovium. It is possible that we cannot detect changes in the lining layer, because 16 weeks after DMM surgery, synovial inflammation is very limited (54), and since we detected very little innervation in the medial synovial lining layer to begin with, it is difficult to demonstrate a further decrease. While nerve sprouting has to our knowledge not yet been reported in experimental OA models, it has been shown that injection of complete Freund's adjuvant into the murine knee resulted in neuronal sprouting in the synovium (55, 56). It will be key to identify the factors that mediate this neuronal growth. One potential candidate is the neurotrophin, Nerve Growth Factor (NGF), which can promote nociceptor sprouting (57). Ongoing clinical trials with neutralizing antibodies against NGF are showing great promise for the treatment of OA pain (58).

The observations reported in this study are purely descriptive, but we propose they will greatly aid in building a coherent approach to the study of the nature of OA joint pain. Our findings in the DMM model illustrate that extensive remodeling of the intra-articular nociceptive innervation of the knee is very much part of the OA disease process, and occurs in different joint tissues. An important question is how the changes we have observed relate to OA pain? Using *in vivo* Ca^{2+}-imaging, we have previously demonstrated that OA is associated with the functional recruitment of a group of joint afferents (20). It is likely that these represent "silent nociceptors" recruited under these circumstances. Characterizing these neurons is clearly of interest for understanding of the anatomical basis for OA pain. Understanding of the genesis of OA joint pain must be based on the innervation of the arthritic joint rather than the normal pattern of innervation. An important question is whether any of the plastic changes in knee innervation observed in OA, for example the neurons present in the subchondral bone channels, correspond to newly functionally recruited nociceptors. If this is the case, they would provide a defined target for therapeutic intervention in OA pain.

Supplementary Material

Refer to Web version on PubMed Central for supplementary material.

Acknowledgements

The authors would like to thank Mr. Shingo Ishihara for performing DMM surgeries and von Frey testing.

Funding: Anne-Marie Malfait (R01AR064251, R01AR060364, R61AR073576) and Richard Miller (R01AR064251, R61AR073576) were supported by the US National Institutes of Health/National Institute of Arthritis and Musculoskeletal and Skin Diseases (NIH/NIAMS). Rachel Miller was supported by NIAMS (K01AR070328). The funding sources had no role in the study.

REFERENCES

1. Lawrence RC, Felson DT, Helmick CG, Arnold LM, Choi H, Deyo RA, et al. Estimates of the prevalence of arthritis and other rheumatic conditions in the United States. Part II. Arthritis Rheum. 2008;58(1):26–35. [PubMed: 18163497]
2. Syx D, Tran PB, Miller RE, Malfait AM. Peripheral Mechanisms Contributing to Osteoarthritis Pain. Curr Rheumatol Rep. 2018;20(2):9. [PubMed: 29480410]
3. Heppelmann B. Anatomy and histology of joint innervation. J Peripher Nerv Syst. 1997;2(1):5–16. [PubMed: 10975732]
4. Loeser RF, Goldring SR, Scanzello CR, Goldring MB. Osteoarthritis: a disease of the joint as an organ. Arthritis Rheum. 2012;64(6):1697–707. [PubMed: 22392533]
5. Little CB, Hunter DJ. Post-traumatic osteoarthritis: from mouse models to clinical trials. Nat Rev Rheumatol. 2013;9(8):485–97. [PubMed: 23689231]
6. Miller RE, Tran PB, Obeidat AM, Raghu P, Ishihara S, Miller RJ, et al. The Role of Peripheral Nociceptive Neurons in the Pathophysiology of Osteoarthritis Pain. Curr Osteoporos Rep. 2015;13(5):318–26. [PubMed: 26233284]
7. Li G, Yin J, Gao J, Cheng TS, Pavlos NJ, Zhang C, et al. Subchondral bone in osteoarthritis: insight into risk factors and microstructural changes. Arthritis Res Ther. 2013;15(6):223. [PubMed: 24321104]
8. Madry H, van Dijk CN, Mueller-Gerbl M. The basic science of the subchondral bone. Knee Surg Sports Traumatol Arthrosc. 2010;18(4):419–33. [PubMed: 20119671]
9. McDougall JJ, Bray RC, Sharkey KA. Morphological and immunohistochemical examination of nerves in normal and injured collateral ligaments of rat, rabbit, and human knee joints. Anat Rec. 1997;248(1):29–39. [PubMed: 9143665]
10. Samuel EP. The autonomic and somatic innervation of the articular capsule. Anat Rec. 1952;113(1):53–70. [PubMed: 14924262]
11. Skoglund S. Anatomical and physiological studies of knee joint innervation in the cat. Acta Physiol Scand Suppl. 1956;36(124):1–101.
12. Gautron L, Sakata I, Udit S, Zigman JM, Wood JN, Elmquist JK. Genetic tracing of Nav1.8-expressing vagal afferents in the mouse. J Comp Neurol. 2011;519(15):3085–101. [PubMed: 21618224]
13. Shields SD, Ahn HS, Yang Y, Han C, Seal RP, Wood JN, et al. Nav1.8 expression is not restricted to nociceptors in mouse peripheral nervous system. Pain. 2012;153(10):2017–30. [PubMed: 22703890]
14. Basbaum AI, Bautista DM, Scherrer G, Julius D. Cellular and molecular mechanisms of pain. Cell. 2009;139(2):267–84. [PubMed: 19837031]
15. Stirling LC, Forlani G, Baker MD, Wood JN, Matthews EA, Dickenson AH, et al. Nociceptor-specific gene deletion using heterozygous NaV1.8-Cre recombinase mice. Pain. 2005;113(1–2):27–36. [PubMed: 15621361]
16. Madisen L, Zwingman TA, Sunkin SM, Oh SW, Zariwala HA, Gu H, et al. A robust and high-throughput Cre reporting and characterization system for the whole mouse brain. Nat Neurosci. 2010;13(1):133–40. [PubMed: 20023653]
17. Jayaraj ND, Bhattacharyya BJ, Belmadani AA, Ren D, Rathwell CA, Hackelberg S, et al. Reducing CXCR4-mediated nociceptor hyperexcitability reverses painful diabetic neuropathy. J Clin Invest. 2018;128(6):2205–25. [PubMed: 29533926]
18. Kim YS, Anderson M, Park K, Zheng Q, Agarwal A, Gong C, et al. Coupled Activation of Primary Sensory Neurons Contributes to Chronic Pain. Neuron. 2016;91(5):1085–96. [PubMed: 27568517]

19. Kim YS, Chu Y, Han L, Li M, Li Z, LaVinka PC, et al. Central terminal sensitization of TRPV1 by descending serotonergic facilitation modulates chronic pain. Neuron. 2014;81(4):873–87. [PubMed: 24462040]
20. Miller RE, Kim YS, Tran PB, Ishihara S, Dong X, Miller RJ, et al. Visualization of Peripheral Neuron Sensitization in a Surgical Mouse Model of Osteoarthritis by In Vivo Calcium Imaging. Arthritis Rheumatol. 2018;70(1):88–97. [PubMed: 28992367]
21. Glasson SS, Blanchet TJ, Morris EA. The surgical destabilization of the medial meniscus (DMM) model of osteoarthritis in the 129/SvEv mouse. Osteoarthritis Cartilage. 2007;15(9):1061–9. [PubMed: 17470400]
22. Miller RE, Tran PB, Das R, Ghoreishi-Haack N, Ren D, Miller RJ, et al. CCR2 chemokine receptor signaling mediates pain in experimental osteoarthritis. Proc Natl Acad Sci U S A. 2012;109(50):20602–7. [PubMed: 23185004]
23. Dixon WJ. Efficient analysis of experimental observations. Annu Rev Pharmacol Toxicol. 1980;20:441–62. [PubMed: 7387124]
24. Chaplan SR, Bach FW, Pogrel JW, Chung JM, Yaksh TL. Quantitative assessment of tactile allodynia in the rat paw. J Neurosci Methods. 1994;53(1):55–63. [PubMed: 7990513]
25. Tran PB, Banisadr G, Ren D, Chenn A, Miller RJ. Chemokine receptor expression by neural progenitor cells in neurogenic regions of mouse brain. J Comp Neurol. 2007;500(6):1007–33. [PubMed: 17183554]
26. Eitner A, Pester J, Nietzsche S, Hofmann GO, Schaible HG. The innervation of synovium of human osteoarthritic joints in comparison with normal rat and sheep synovium. Osteoarthritis Cartilage. 2013;21(9):1383–91. [PubMed: 23973153]
27. Karanth SS, Dhital S, Springall DR, Polak JM. Reinnervation and neuropeptides in mouse skin flaps. J Auton Nerv Syst. 1990;31(2):127–34. [PubMed: 2149731]
28. Ramieri G, Anselmetti GC, Baracchi F, Panzica GC, Viglietti-Panzica C, Modica R, et al. The innervation of human teeth and gingival epithelium as revealed by means of an antiserum for protein gene product 9.5 (PGP 9.5). Am J Anat. 1990;189(2):146–54. [PubMed: 2147092]
29. Miller RE, Tran PB, Ishihara S, Larkin J, Malfait AM. Therapeutic effects of an anti-ADAMTS-5 antibody on joint damage and mechanical allodynia in a murine model of osteoarthritis. Osteoarthritis Cartilage. 2016;24(2):299–306. [PubMed: 26410555]
30. Ivanusic JJ. Molecular Mechanisms That Contribute to Bone Marrow Pain. Front Neurol. 2017;8:458. [PubMed: 28955292]
31. Mach DB, Rogers SD, Sabino MC, Luger NM, Schwei MJ, Pomonis JD, et al. Origins of skeletal pain: sensory and sympathetic innervation of the mouse femur. Neuroscience. 2002;113(1):155–66. [PubMed: 12123694]
32. Jimenez-Andrade JM, Mantyh WG, Bloom AP, Xu H, Ferng AS, Dussor G, et al. A phenotypically restricted set of primary afferent nerve fibers innervate the bone versus skin: therapeutic opportunity for treating skeletal pain. Bone. 2010;46(2):306–13. [PubMed: 19766746]
33. Verdu E, Ceballos D, Vilches JJ, Navarro X. Influence of aging on peripheral nerve function and regeneration. J Peripher Nerv Syst. 2000;5(4):191–208. [PubMed: 11151980]
34. Ceballos D, Cuadras J, Verdu E, Navarro X. Morphometric and ultrastructural changes with ageing in mouse peripheral nerve. J Anat. 1999;195 (Pt 4):563–76. [PubMed: 10634695]
35. Chang YC, Lin WM, Hsieh ST. Effects of aging on human skin innervation. Neuroreport. 2004;15(1):149–53. [PubMed: 15106848]
36. Kenshalo DR Sr. Somesthetic sensitivity in young and elderly humans. J Gerontol. 1986;41(6): 732–42. [PubMed: 3772049]
37. Assimakopoulos AP, Katonis PG, Agapitos MV, Exarchou EI. The innervation of the human meniscus. Clin Orthop Relat Res. 1992(275):232–6. [PubMed: 1735219]
38. Salo PT, Tatton WG. Age-related loss of knee joint afferents in mice. J Neurosci Res. 1993;35(6): 664–77. [PubMed: 8411268]
39. Salo PT, Seeratten RA, Erwin WM, Bray RC. Evidence for a neuropathic contribution to the development of spontaneous knee osteoarthrosis in a mouse model. Acta Orthop Scand. 2002;73(1):77–84. [PubMed: 11928917]

40. Chartier SR, Mitchell SAT, Majuta LA, Mantyh PW. The Changing Sensory and Sympathetic Innervation of the Young, Adult and Aging Mouse Femur. Neuroscience. 2018;387:178–90. [PubMed: 29432884]
41. McNulty MA, Loeser RF, Davey C, Callahan MF, Ferguson CM, Carlson CS. Histopathology of naturally occurring and surgically induced osteoarthritis in mice. Osteoarthritis Cartilage. 2012;20(8):949–56. [PubMed: 22595226]
42. Nagelli CV, Cook JL, Kuroki K, Bozynski C, Ma R, Hewett TE. Does Anterior Cruciate Ligament Innervation Matter for Joint Function and Development of Osteoarthritis? J Knee Surg. 2017;30(4):364–71. [PubMed: 27648746]
43. Dye SF, Vaupel GL, Dye CC. Conscious neurosensory mapping of the internal structures of the human knee without intraarticular anesthesia. Am J Sports Med. 1998;26(6):773–7. [PubMed: 9850777]
44. Suri S, Gill SE, Massena de Camin S, Wilson D, McWilliams DF, Walsh DA. Neurovascular invasion at the osteochondral junction and in osteophytes in osteoarthritis. Ann Rheum Dis. 2007;66(11):1423–8. [PubMed: 17446239]
45. Mapp PI, Walsh DA. Mechanisms and targets of angiogenesis and nerve growth in osteoarthritis. Nat Rev Rheumatol. 2012;8(7):390–8. [PubMed: 22641138]
46. Ashraf S, Wibberley H, Mapp PI, Hill R, Wilson D, Walsh DA. Increased vascular penetration and nerve growth in the meniscus: a potential source of pain in osteoarthritis. Ann Rheum Dis. 2011;70(3):523–9. [PubMed: 21081524]
47. Mapp PI, Avery PS, McWilliams DF, Bowyer J, Day C, Moores S, et al. Angiogenesis in two animal models of osteoarthritis. Osteoarthritis Cartilage. 2008;16(1):61–9. [PubMed: 17659886]
48. Mapp PI, Sagar DR, Ashraf S, Burston JJ, Suri S, Chapman V, et al. Differences in structural and pain phenotypes in the sodium monoiodoacetate and meniscal transection models of osteoarthritis. Osteoarthritis Cartilage. 2013;21(9):1336–45. [PubMed: 23973148]
49. Murakami K, Nakagawa H, Nishimura K, Matsuo S. Changes in peptidergic fiber density in the synovium of mice with collagenase-induced acute arthritis. Can J Physiol Pharmacol. 2015;93(6): 435–41. [PubMed: 25909759]
50. Buma P, Verschuren C, Versleyen D, Van der Kraan P, Oestreicher AB. Calcitonin gene-related peptide, substance P and GAP-43/B-50 immunoreactivity in the normal and arthrotic knee joint of the mouse. Histochemistry. 1992;98(5):327–39. [PubMed: 1283163]
51. Aso K, Izumi M, Sugimura N, Okanoue Y, Ushida T, Ikeuchi M. Nociceptive phenotype alterations of dorsal root ganglia neurons innervating the subchondral bone in osteoarthritic rat knee joints. Osteoarthritis Cartilage. 2016;24(9):1596–603. [PubMed: 27085969]
52. Ferreira-Gomes J, Adaes S, Sarkander J, Castro-Lopes JM. Phenotypic alterations of neurons that innervate osteoarthritic joints in rats. Arthritis Rheum. 2010;62(12):3677–85. [PubMed: 20722015]
53. Thakur M, Rahman W, Hobbs C, Dickenson AH, Bennett DL. Characterisation of a peripheral neuropathic component of the rat monoiodoacetate model of osteoarthritis. PLoS One. 2012;7(3):e33730. [PubMed: 22470467]
54. Jackson MT, Moradi B, Zaki S, Smith MM, McCracken S, Smith SM, et al. Depletion of protease-activated receptor 2 but not protease-activated receptor 1 may confer protection against osteoarthritis in mice through extracartilaginous mechanisms. Arthritis Rheumatol. 2014;66(12): 3337–48. [PubMed: 25200274]
55. Ghilardi JR, Freeman KT, Jimenez-Andrade JM, Coughlin KA, Kaczmarska MJ, Castaneda-Corral G, et al. Neuroplasticity of sensory and sympathetic nerve fibers in a mouse model of a painful arthritic joint. Arthritis Rheum. 2012;64(7):2223–32. [PubMed: 22246649]
56. Jimenez-Andrade JM, Mantyh PW. Sensory and sympathetic nerve fibers undergo sprouting and neuroma formation in the painful arthritic joint of geriatric mice. Arthritis Res Ther. 2012;14(3):R101. [PubMed: 22548760]
57. Denk F, Bennett DL, McMahon SB. Nerve Growth Factor and Pain Mechanisms. Annu Rev Neurosci. 2017;40:307–25. [PubMed: 28441116]
58. Miller RE, Block JA, Malfait AM. What is new in pain modification in osteoarthritis? Rheumatology (Oxford). 2018;57(suppl_4):iv99–iv107. [PubMed: 29361112]

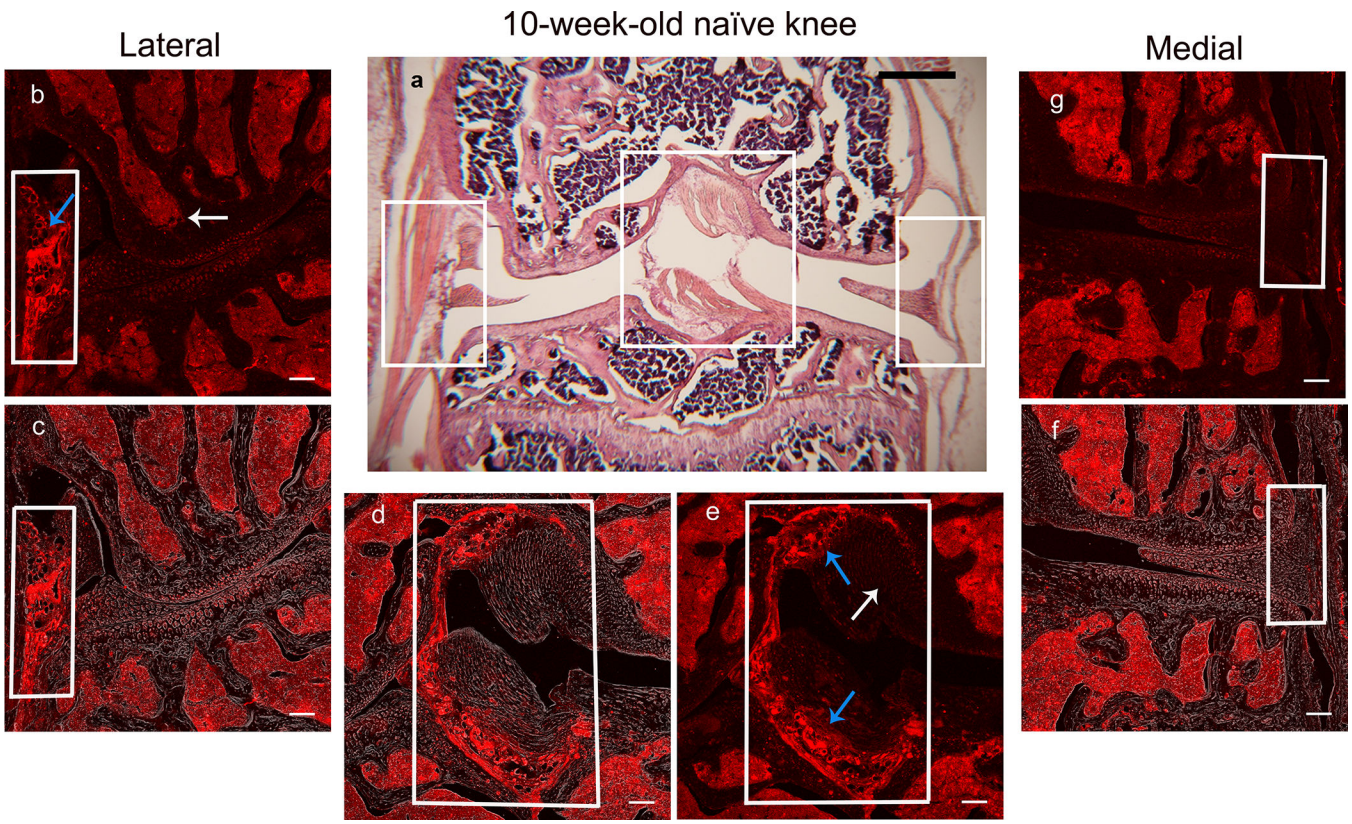

Figure 1.

Representative histological images of the right knee joint of a 10-week-old $Na_V1.8$-tdTomato mouse. (a) H&E staining. Scale bar = 500 μm; (b,e,g) Confocal images of $Na_V1.8$-tdTomato expressing afferent nerve fibers within the lateral, middle, and medial parts of the knee joint, respectively. In (b), the blue arrow indicates dense innervation within the lateral synovium and the white arrow indicates dense innervation in the bone marrow. In (e), the blue arrows indicate dense innervation in the connective tissue surrounding the cruciate ligaments and at the insertion sites, while the white arrow indicates the substance of cruciate ligament; (c,d,f) Overlays of the $Na_V1.8$-tdTomato images with phase-contrast to show the general structures of the joint; (b-g) Scale bar = 100 μm.

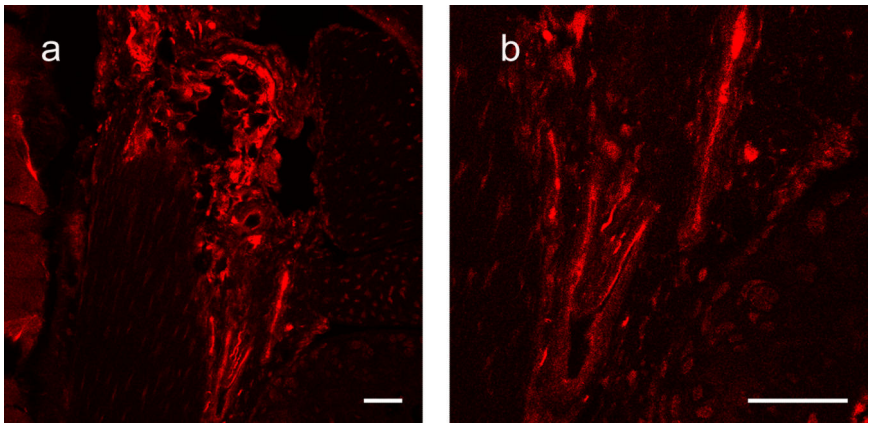

Figure 2.

Nikon A1R confocal images showing the lateral side of a 10-week old $Na_V1.8$-tdTomato mice. (a) Confocal image shows the $Na_V1.8$+ fibers within the lateral synovium. Magnified image of these fibers is shown in (b). Scale bar = 50 μm.

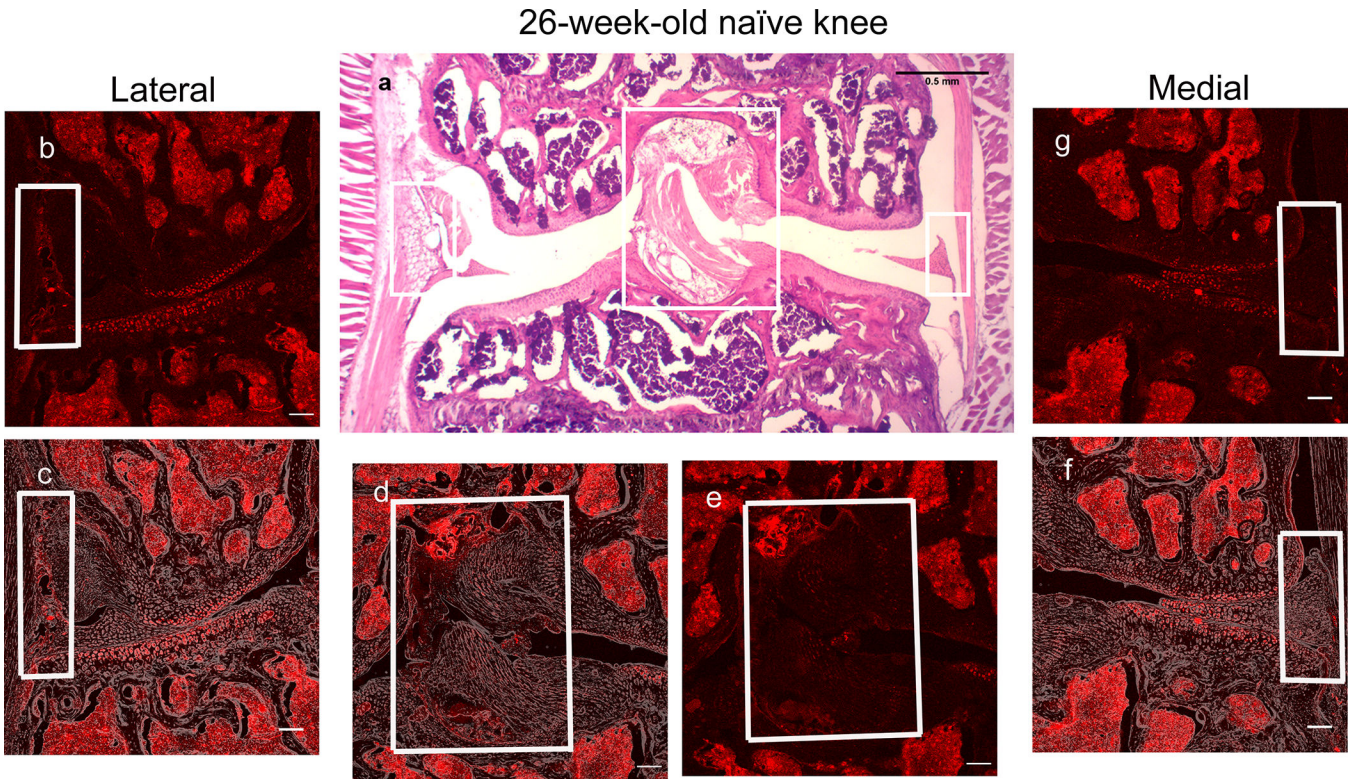

Figure 3.

Representative histological images of the right knee joint of a 26-week-old $Na_V1.8$-tdTomato mouse. (a) H&E staining. Scale bar = 500 μm; (b,e,g) Confocal images of $Na_V1.8$-tdTomato expressing afferent nerve fibers within the lateral, middle, and medial parts of the knee joint, respectively; (c,d,f) Overlays of the $Na_V1.8$-tdTomato images with phase-contrast to show the general structures of the joint; (b-g) Scale bar = 100 μm.

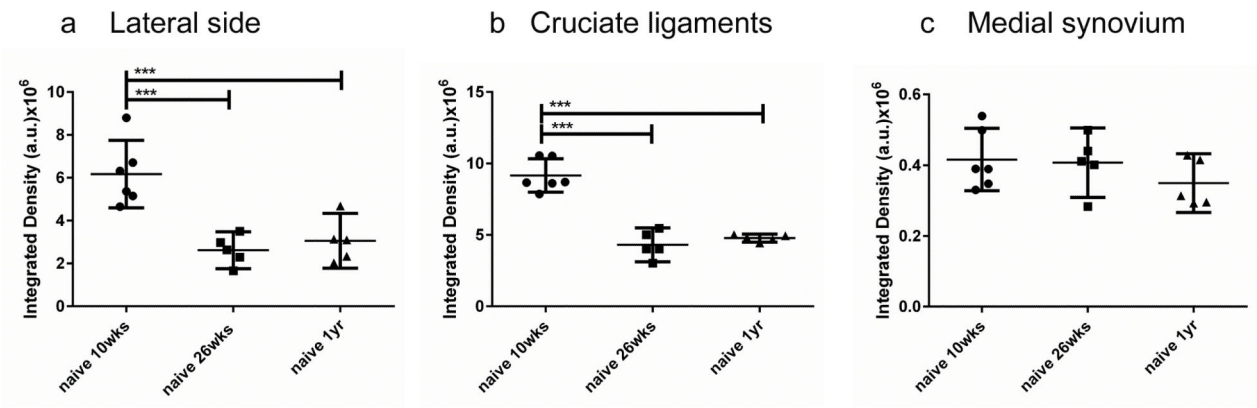

Figure 4.

Quantification of $Na_V1.8$-tdTomato signal in knees from 10-week (n=6), 26-week (n=5) and 1-year old mice (n=5), in (a) the lateral synovium and meniscus; (b) the cruciate ligaments, and (c) the medial synovium. *** $p < 0.001$. mean ± 95% CI.

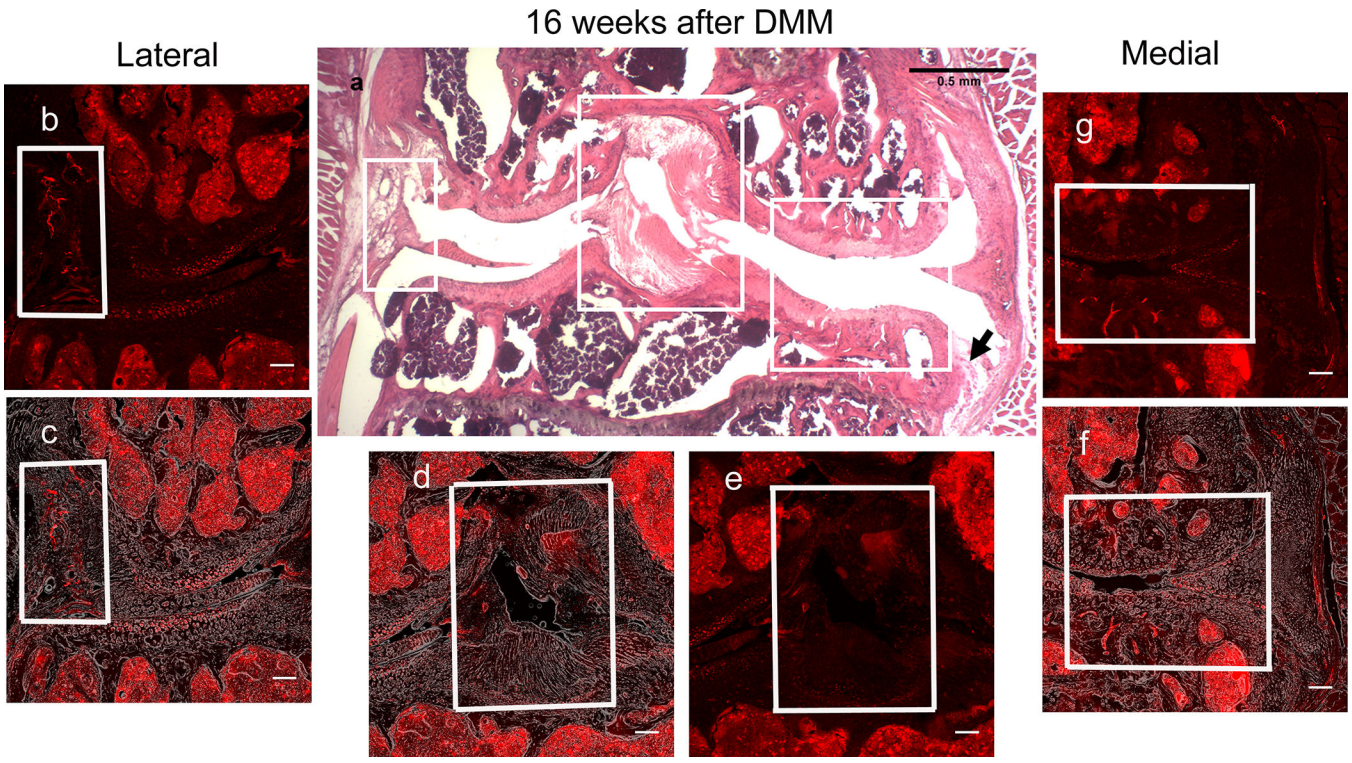

Figure 5.

Representative histological images of the right knee joint 16 weeks after DMM surgery. (a) H&E image showing cartilage degradation and subchondral bone sclerosis in the medial compartment. The black arrow indicates an osteophyte. Scale bar = 500 μm; (b,e,g) Confocal images of $Na_V1.8$-tdTomato expressing afferent nerve fibers within the lateral, middle, and medial parts of the knee joint, respectively. In (g) and (f), note the channels containing $Na_V1.8$+ neurons in the medial tibial plateau and femoral condyle (within the white box). Blue arrows in (g) shows the $Na_V1.8$-tdTomato expressing afferents in the medial synovium; (c,d,f) Overlays of the $Na_V1.8$-tdTomato images with phase-contrast to show the general structures of the joint; (b-g) Scale bar = 100 μm.

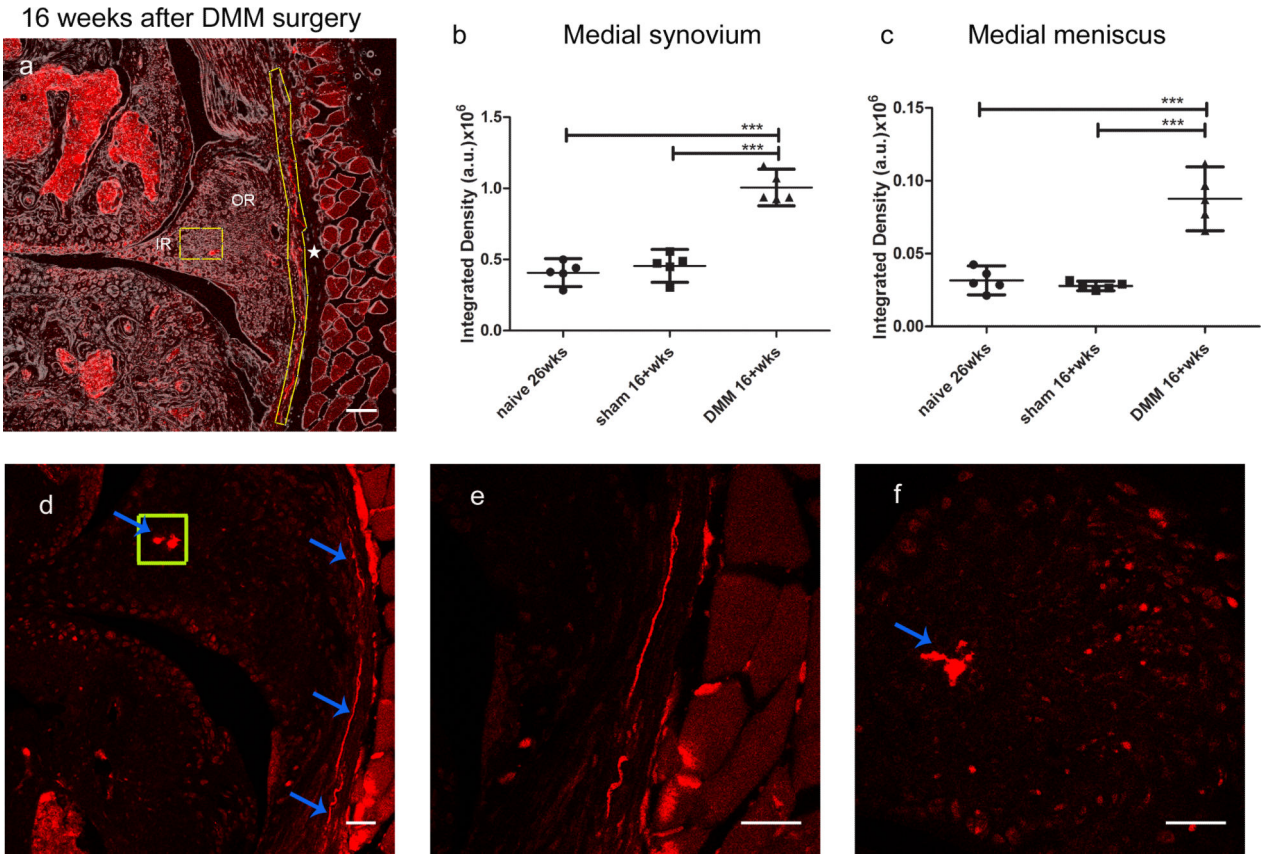

Figure 6.

(a) Confocal image showing $Na_V1.8$-tdTomato expressing afferent nerve fibers in the medial synovium in the DMM knee (yellow outline next to the star). $Na_V1.8$ signal was also observed in the outer region of the medial meniscus of DMM knees, close to the junction of outer (OR) and inner region (IR) (yellow box). The star indicates the capsule; (b,c) Quantification of $Na_V1.8$ tdTomato signal in knees from 26-week old naïve mice, and mice 16 weeks after sham or DMM surgery (n=5/group), in (b) the medial synovium and (c) the medial meniscus; *** $p < 0.001$. Scale bar = 100 μm. (d-f) Nikon A1R confocal images showing similar features: (d) shows $Na_V1.8$+ fibers in the medial synovium (blue arrows, e shows that area magnified) and the $Na_V1.8$ positive signal inside the medial meniscus (shown in the yellow box, f shows magnified image of the signal). Scale bar = 50 μm. mean ± 95% CI.

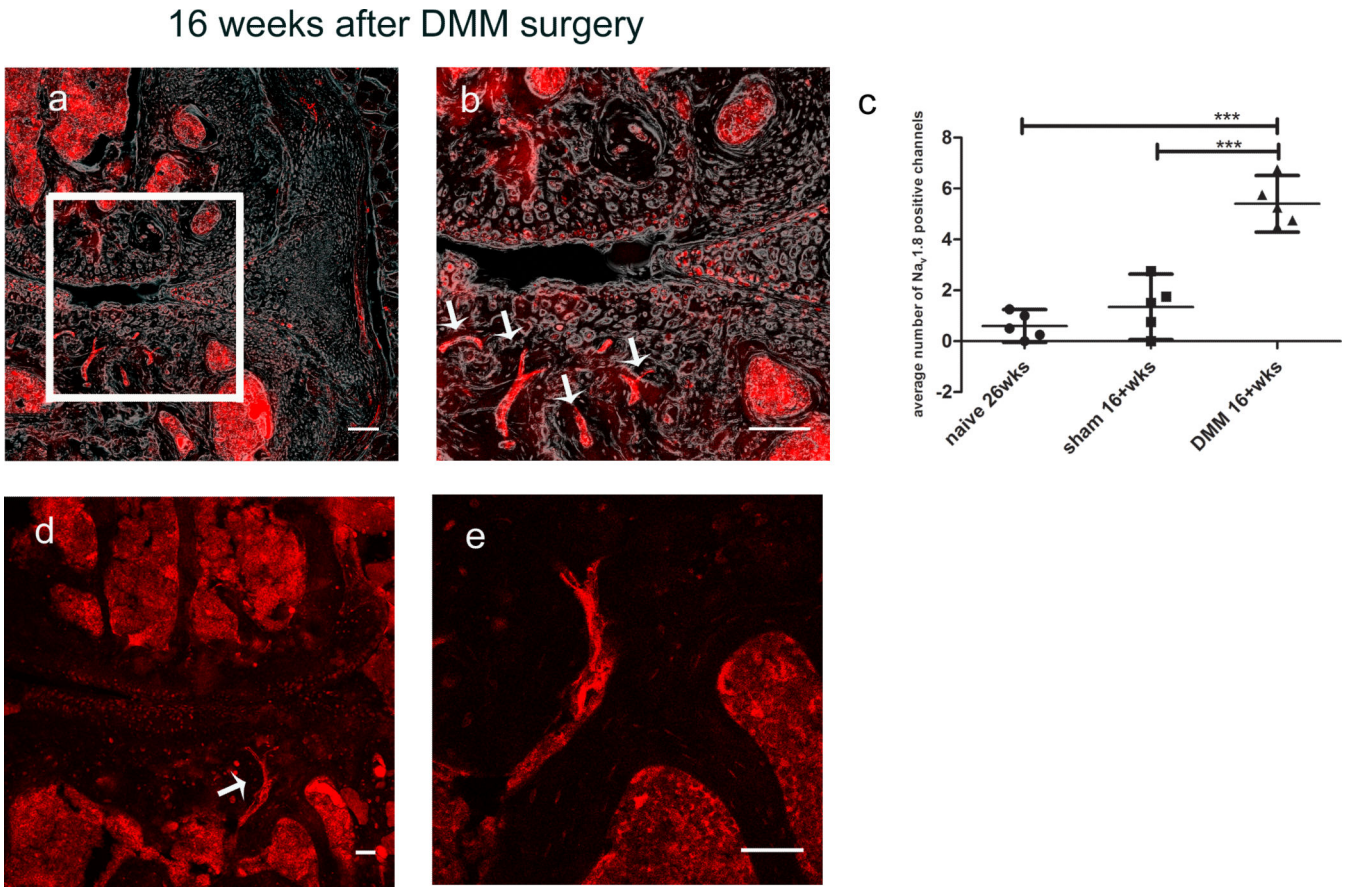

Figure 7.

(a) Confocal image of a right knee joint 16 weeks after DMM surgery shows subchondral bone channels in the medial tibial plateau, with nerves in the subchondral bone pointing toward the calcified cartilage (white inset); (b) Magnified image, with the arrows pointing at $Na_V1.8$+ neurons; (c) Quantification of $Na_V1.8$ tdTomato positive channels in the subchondral bone of tibial plateaux and femoral condyles from 26-week old naïve mice, and 16 weeks after sham or DMM surgery (n=5/group). *** $p < 0.001$. mean ± 95% CI. (a-b) Scale bar = 100 μm. (d) Nikon A1R confocal image shows $Na_V1.8$ expressing nerve fibers within a subchondral bone channel; (e) shows a magnified image of these fibers; this image also shows the punctate $Na_V1.8$ signal inside the bone marrow cavities. Scale bar = 50 μm.

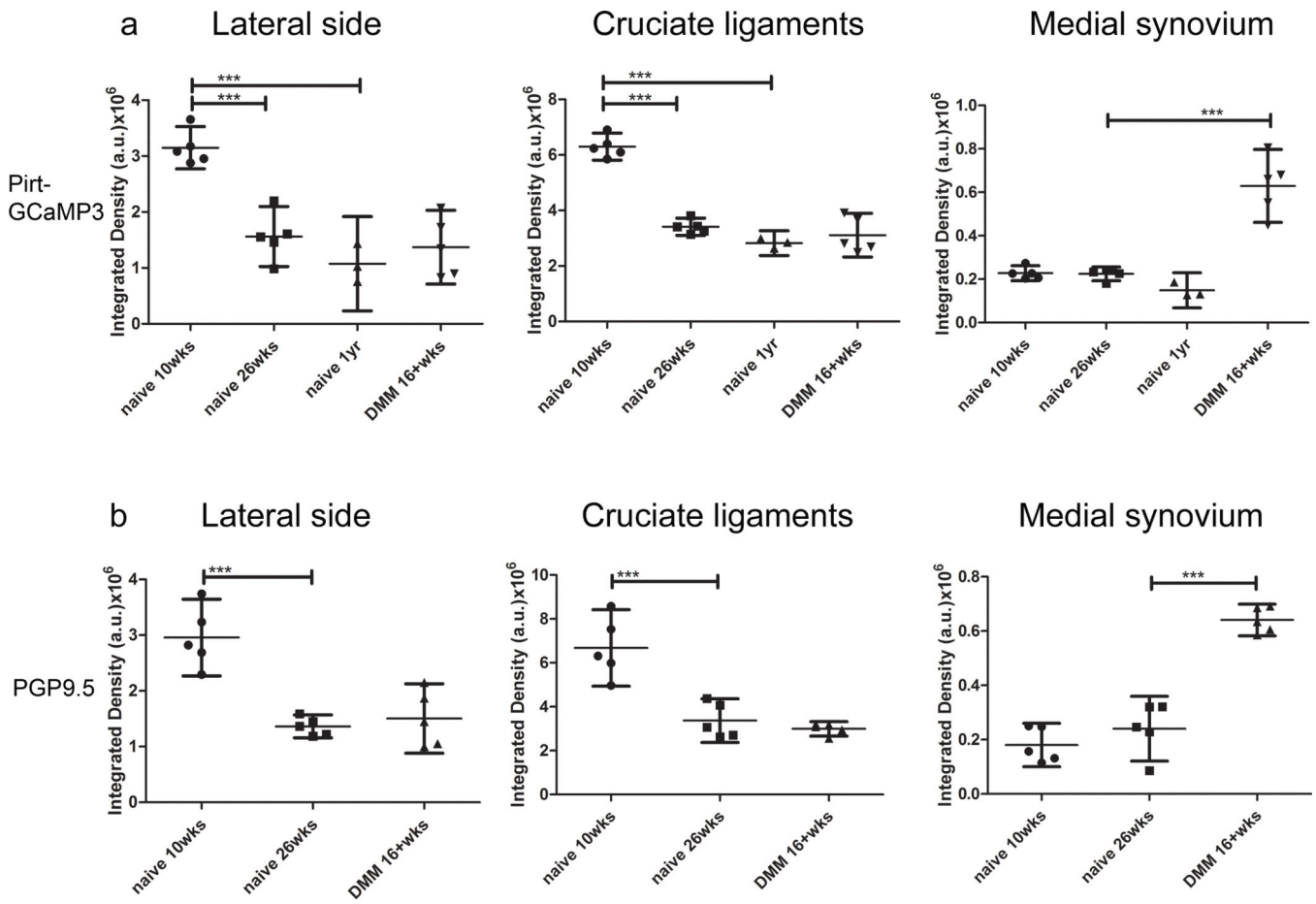

Figure 8.

(a) Quantification of GCaMP3 signal in knees from 10-week old naïve Pirt-GCaMP3 mice (n=5), 26-week old naïve mice (n=5), 1-year old naïve mice (n=3), and from mice 16 weeks after DMM surgery (n=5) in the lateral synovium and meniscus, the cruciate ligaments and medial synovium; (b) Quantification of PGP9.5 signal in WT knees from n=5 mice for each different group (10-week old, 26-week old naïve mice and 16 weeks after DMM surgery) in the lateral synovium and meniscus, the cruciate ligaments and medial synovium. *** $p < 0.001$. mean ± 95%CI